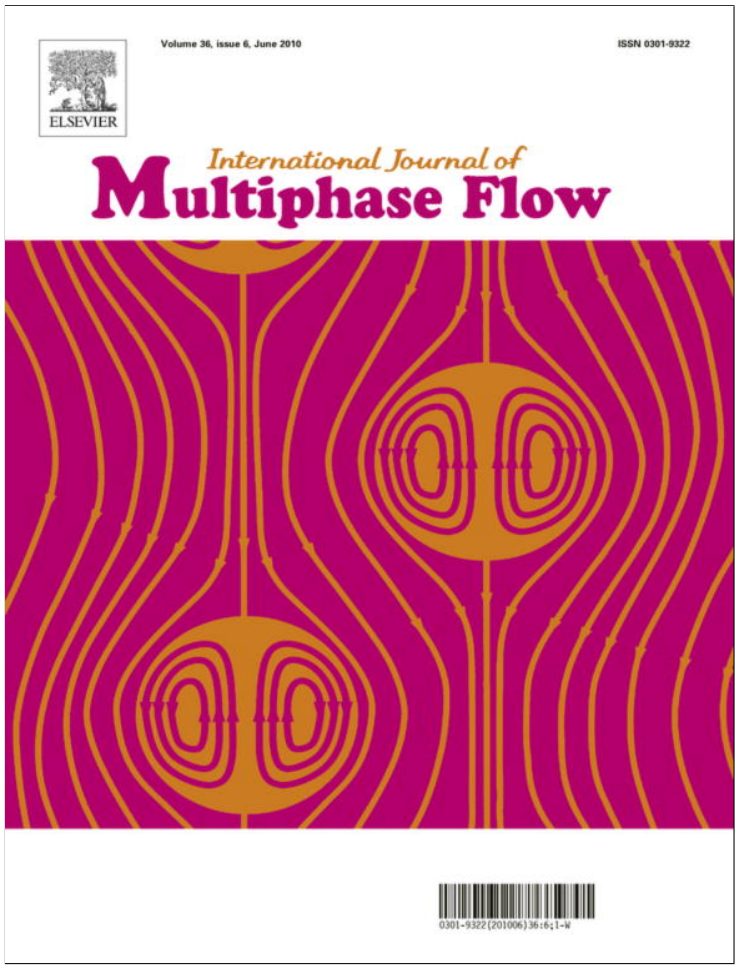

International Journal of Multiphase Flow 36 (2010) 481–490

Contents lists available at ScienceDirect

International Journal of Multiphase Flow

journal homepage: www.elsevier.com/locate/ijmulflow

Sedimentation of bidisperse suspensions

Robert Dorrell, Andrew J. Hogg *

Centre for Environmental and Geophysical Flows, School of Mathematics, University Walk, University of Bristol, BS8 1TW, UK

ARTICLE INFO

Article history:
Received 27 October 2009
Received in revised form 1 February 2010
Accepted 3 February 2010
Available online 10 February 2010

Keywords:
Sedimentation
Deposition
Bidisperse
Mass conservation
Method of characteristics

ABSTRACT

The average settling velocity of a suspension of identical particles through otherwise quiescent fluid is smaller than the settling velocity of a single particle in an unbounded fluid. When a suspension settles out to form a deposit, this hindered settling effect may lead to complicated sedimentation behaviour, even if the initial suspension is uniformly distributed. This study analyses the bulk sedimentation of bidisperse suspensions and calculates the evolution of the volume fraction of each species from an initially vertically uniform state through to the final steady state where both species have fully settled out of suspension and have formed a deposit. These calculations are analytical and employ the method of characteristics to reveal how both particle species evolve. The profiles often include 'shocks', across which discontinuous changes in volume fraction occur. Rarefaction fans may also be found across which the gradients of volume fraction are discontinuous. These new analytical solutions reveal the evolving composition of the suspension and the deposit and may be compared to experimental observations. They also provide test cases that can be used to verify recent numerical techniques for computing the bulk sedimentation behaviour of polydisperse suspensions.

1. Introduction

Understanding sedimentation from polydisperse suspensions of relatively dense particles is of considerable importance for particulate flows in many industrially and naturally-occurring situations. Very often direct measurements of the settling processes are not possible and inferences must be drawn by analysing the composition of the resulting deposit. In this paper we model mathematically the sedimentation of bidisperse suspensions through otherwise quiescent fluid and analyse in detail the structure of the deposit they generate, relating its composition to material properties of the constituent particles and initial properties of the suspension.

A suspension will generally comprise of particles with a range of sizes and densities and this implies that there will be a range of settling velocities. There is a large body of research into the dynamics of polydisperse sedimentation featuring both experimental and theoretical approaches. This research has principally addressed either the problem of sedimentation velocity of a given particle in suspension, or the bulk sedimentation behaviour, which describes the settling and depositional behaviour of the entire suspension, for all particle species.

Recent experiments have introduced novel techniques for measuring the evolution of particulate suspensions and associated deposit, when the concentration of suspended particles is high. For example acoustic techniques (Hoyos et al., 1994) and nuclear magnetic resonance (NMRI) (Cheung et al., 1994) have been used to measure concentration profiles of sedimenting particles. The acoustic method yields accurate measurements of the suspensions at volumetric concentrations of up to 50%, whilst using NMRI the concentration of the suspension can be accurately measured up to and including the maximum packing value. These techniques have been used to give a complete profile of the temporally evolving, concentration of particulates. From these experiments velocities of settling interfaces of different particle species were inferred and compared to theoretical predictions made by Selim et al. (1983) and Davis and Gecol (1994). However, as both of these techniques have only been used to resolve the total concentration profile, we cannot use them to infer the behaviour of interior dynamics, such as rising shocks in particle concentrations which, as will be shown in this paper, are strongly dependent on the concentrations of individual particle species.

Amy et al. (2006) provided measurements of the deposit structure from sedimenting polydisperse suspensions and showed that the deposit structure maybe related to the initial conditions of the suspension. Our results demonstrate that any variations in individual particle concentrations during sedimentation will be recorded in the deposit as the particles settle out and thus the deposit structure is an important method for inferring the bulk sedimentation behaviour of a given suspension.

While the Stokesian settling velocity of an individual particle through unbounded viscous fluid is well established (Batchelor,

* Corresponding author.
E-mail addresses: rob.dorrell@bris.ac.uk (R. Dorrell), a.j.hogg@bris.ac.uk (A.J. Hogg).

0301-9322/$ - see front matter © 2010 Elsevier Ltd. All rights reserved.
doi:10.1016/j.ijmultiphaseflow.2010.02.001

1967), the settling velocity at high concentrations and of mixtures of particle sizes remains on a less firm theoretical footing. The problem can be summarised as a reduction of Stokesian settling velocity with an increase in concentration due to the combined effects of viscosity enhancement by the presence of nearby particles (Richardson and Zaki, 1954) and the interstitial fluid flow generated by the motion of the surrounding particles. In this context, various 'hindered settling' laws have been proposed to account for these effects.

Batchelor (1982) introduced a settling law which used a complex sedimentation expression and a mass conservation model to describe the settling velocity of a particle in a dilute suspension. The sedimentation model was derived in terms of submerged gravitational forces, Van der Waals forces and the relative diffusion for a pair of particles. The relative position of the particles was modelled probabilistically and was dependent on material properties of the particles (ratios of diameters and densities), the ratio of relative motion due to van der Waals forces and Brownian diffusion and the particle Péclet number, *Pe*, which measures ratio of advection to diffusion. Several similar settling laws have been proposed, which agree in the dilute limit with Batchelor's but extend the model higher concentrations (with greater accuracy) (Davis and Gecol, 1994; Koo, 2009).

An alternative approach to modelling non-cohesive polydisperse suspensions was developed by Masliyah (1979) and Lockett and Bassoon (1979). This empirical model, henceforth referred to as the MLB model, includes the aforementioned viscosity enhancement due to high concentrations of particles and a mass balance from the return flow of water generated due to the motion of nearby particles. It is of similar form to the Batchelor settling velocity when diffusion and van der Waals forces are negligible in comparison to the gravitational force and is described in more detail in Section 2.1. An often used validation technique of the Batchelor and MLB settling velocity models is to calculate and compare against experiments measuring the fall velocity of different interfaces separating regions of different particle distributions, see for example Lockett and Bassoon (1979), Selim et al. (1983).

In this paper we use the MLB expression for our hindered settling law. The simplified MLB expression is chosen as it has been shown to have reasonable success at capturing the fall velocities of interfaces of non cohesive bi- and polydisperse suspensions (Lockett and Al-Habbooby, 1973; Xue and Sun, 2002), which are the focus of this paper. Modelling the settling velocity of suspensions comprising cohesive, or mixtures of cohesive and non-cohesive, particles requires more complex sedimentation laws to account for all the forces acting on a settling particle (Cuthbertson et al., 2008). Here we restrict the study to particle suspensions where cohesive forces may be assumed negligible. Although the MLB model has been widely used (Basson et al., 2009) it has been criticised for not capturing the stronger hindrance of large particles as compared to small particles at very high concentrations ($\phi > 0.45$), as noted by Selim et al. (1983) and Hoyos et al. (1994), where it is proposed that small particles are 'dragged along' by large particles.

Studies of bulk sedimentation are focused on the complete evolution of a suspension within a bounded domain, as it evolves from an initial state through to the final deposit. For monodisperse suspensions, a key contribution was made by Kynch (1952), who showed that by writing the sedimentation velocity as a function of the local volume fraction of particles, a number of important dynamical features could be reproduced in continuum models of the sedimentation process, most notably including 'shocks', in which the local concentration of particles abruptly varies over a vanishing small vertical extent. Kynch's model was essentially derived as an expression of the conservation of particulate mass – momentum and, in particular, inertia of the particles were not explicitly modelled. Auzerais et al. (1988) presented a more complete model of the dynamics of sedimentation, including inertia and stress generation due to contacts and showed that discontinuities in particle concentration became smoothed out as Péclet number was decreased. However at large Péclet numbers it was shown that predicted concentration profiles exhibited Kynch-like behaviour. For sand-sized particles, typically hundreds of microns in diameter, suspended in water, the Péclet number is large enough for inertial effects to be ignored (typically $Pe \approx 10^9$).

Recent work by Bürger et al. (2000) and Bürger et al. (2008) has developed a range finite element numerical algorithms for the Kynch (1952) continuum models. They have extended the models to cope with bi- and polydisperse suspensions, using a MLB settling law and integrate coupled equations for each particle species independently. The finite element models incorporate various artificial numerical viscosities to cope with shocks in particle concentration. The numerical results have been shown to reproduce experimentally measured sedimentation behaviour (Basson et al., 2009).

The aforementioned work by Kynch and Burger model the bulk behaviour of the suspension assuming a horizontally homogeneous suspension of particles. However, as shown by Batchelor and Rensburg (1984) and Funamizu and Takakuwa (1996), structure formation in a sedimenting suspension of particle may form density-driven instabilities in the sedimenting media. These structures manifest themselves as high concentration clumping driving a localised flow which can reinforce the clumping behaviour and greatly distort the predicted sedimentation behaviour. They are shown to arise, under certain conditions, from horizontal perturbations to homogeneous particle suspensions (Batchelor and Rensburg, 1984). In the following work we restrict ourselves, as Kynch did, to modelling vertical variations in particle concentration and therefore do not include these effects.

We note that although there have been many theoretical studies of the sedimentation velocity of particles in suspension there has been a dearth in theoretical development, numerical analysis aside, of the bulk sedimentation process since Kynch (1952) and it is this issue we tackle in this paper. We review Kynch's contribution in what follows and crucially amend his settling law with one that predicts that all of the particles have settled out of suspension within a finite time (Section 2), a problem Kynch (1952) had noted and attempted to rectify in his original paper. However the main contribution of this study is to analyse bidisperse sedimentation (Section 3). We show that the method of characteristics may be applied to the now coupled settling equations for each of the two species of particles to construct analytical solutions for the volume fraction of each species. This reveals a rich variety of behaviours and structures within the deposit that are functions of the relative sizes, densities and initial concentrations of the suspended particles. However we are able to classify this more complicated settling in an analogous way to monodisperse sedimentation. These results may be used to interpret results from recent laboratory experiments of the settling of mixtures of particles Amy et al. (2006). Furthermore these exact solutions provide test cases to validate numerical schemes for integrating the governing equations, which can then be applied to more complicated sedimentation problems (Bürger et al., 2008).

None of the aforementioned theoretical and numerical work has made predictions on the structure of the deposit formed by sedimenting material. Thus the scope of this paper is threefold: to understand and explain fully the sedimentation behaviour using a justifiable hindered settling law; to relate deposit structure to material properties and initial properties of the suspension; and to provide analytical solutions which can validate numerical models.

2. Sedimentation of monodisperse suspensions

2.1. Particle settling velocity and mass conservation laws

We present a brief summary of the monodisperse version of the particle settling velocity used in the MLB model, see Masliyah (1979) and Lockett and Bassoon (1979). Mass conservation of particulate equates change in particle concentration to the gradient of particle flux. Particle flux is given by the hindered settling velocity of a sedimenting particle species multiplied by the particle species concentration (Kynch, 1952). The model considers the time dependent evolution of the volume fraction of particles, $\phi(z,t)$, where the z-axis is vertically aligned, on the assumption that diffusive effects are negligible. Denoting the vertical velocities of the solid and fluid phases by w_s and w_f, respectively, mass conservation is given by

$$\frac{\partial \phi}{\partial t}+\frac{\partial}{\partial z}(\phi w_s)=0 \quad \text{and} \quad \frac{\partial (1-\phi)}{\partial t}+\frac{\partial}{\partial z}((1-\phi)w_f)=0. \tag{1}$$

Then by summing these two equations, so that the combined vertical mass flux vanishes, we find that

$$w_s=(1-\phi)w_p, \tag{2}$$

where $w_p \equiv w_s - w_f$ is the slip velocity between the particle and fluid phases.

The slip velocity for a single spherical particle of diameter D in an unbounded fluid is readily calculated by equating the vertical component of its submerged weight, $\pi D^3(\rho_s-\rho_f)g/6$, where the densities of the solid and fluid phases and gravitational acceleration are denoted by ρ_s, ρ_f and g, respectively, with the viscous drag, $3\pi\mu D w_p$, where μ is the viscosity of the suspending fluid. This dynamical balance, which is appropriate provided the inertial effects of the fluid remain negligible, yields the Stokes' settling velocity. For a particle in a suspension, we amend this description in two ways. First the viscosity of the suspension is enhanced and following Richardson and Zaki (1954), amongst others, we write the effective viscosity of the suspension as $\mu_e=\mu/(1-\phi)^{n-1}$, where n is determined empirically. Further we assume that once a maximum volume fraction of particulate, ϕ_m is exceeded, then the submerged weight is borne by the solid matrix, so that the slip velocity (and drag) vanish. Together these assumptions imply that the downwards settling velocity of the solid phase is given by

$$w_s=\begin{cases} -w_{s0}(1-\phi)^n & \phi \leqslant \phi_m \\ 0 & \phi > \phi_m \end{cases}, \tag{3}$$

where w_{s0} is the absolute value of the settling velocity for a single particle in unbounded fluid, which is given by the Stokes settling velocity ($[\rho_s-\rho_f]gD^2/[18\mu]$) for a spherical particle. We demonstrate below that this formulation allows the settling velocity of the solid phase to be easily generalised to include bi- and polydisperse suspensions.

2.2. Characteristic solutions for quiescent settling

We write mass conservation (1a) in dimensionless form using the flow depth, h, as a length scale and h/w_{s0} as a timescale. Henceforth dimensionless velocities are distinguished by a carat. Further we denote the vertical flux of particles per unit area by $F=\phi\hat{w}_s$ so that the governing equation is given by

$$\frac{\partial \phi}{\partial T}+\frac{\partial F}{\partial Z}=0, \tag{4}$$

where T and Z are the dimensionless time and vertical coordinate, respectively. This equation is solved subject to a condition of no flux condition at the base of the flow $F(\phi(0,T))=0$ and an initial concentration profile of particulate. Here we impose a vertically uniform concentration profile, so that $\phi(Z,0)=\Theta$, where Θ provides a dimensionless measure of the total amount of sediment in suspension. The governing equation is readily integrated using the method of characteristics, see Kynch (1952) and for further details Whitham (1974), by writing

$$\frac{\mathrm{d}\phi}{\mathrm{d}T}=0 \quad \text{on} \quad \frac{\mathrm{d}Z}{\mathrm{d}T}\equiv\lambda(\phi)=\frac{\partial F}{\partial \phi}. \tag{5}$$

This implies that for monodisperse suspensions, the characteristics are lines of constant concentration. Solutions to this governing equation may exhibit discontinuities ('shocks') over which the concentration changes. The jump condition (Rankine-Hugoniot condition) across the discontinuity may be deduced from the mass conservation equation to give the shock speed, $\dot{S}$, as a function of the volume fractions above and below the shock, denoted by $\phi^+\equiv\phi(S^+,T)$ and $\phi^-\equiv\phi(S^-,T)$, respectively. It is expressed as

$$\dot{S}(T)=\frac{F(\phi^-)-F(\phi^+)}{\phi^- - \phi^+}. \tag{6}$$

The location of the top interface, $\gamma(T)$, and the deposit height, $\eta(T)$, are given by

$$\frac{\mathrm{d}\gamma}{\mathrm{d}T}=\hat{w}_s(\phi(\gamma,T)), \quad \frac{\mathrm{d}\eta}{\mathrm{d}T}=-\frac{\phi\hat{w}_s(\phi)}{\phi_m-\phi}. \tag{7}$$

Both of these can be viewed as shocks; the former is a discontinuity of particle concentration between the top of the settling layer and pure fluid above, whereas the latter is a discontinuity between the stationary deposit and the settling layer, the speed of which is denoted by $\dot{S}_m(\phi)$.

Following Kynch (1952), the interior shock formed is the one that grows with the greatest speed, $\dot{S}_*$. The reasoning for this is simple: if we choose a shock (or characteristic) that grows more slowly it will be immediately over taken by $\dot{S}_*$. Given uniform initial conditions, $\phi^+=\Theta$, the shock speed can therefore be treated as a function of the concentration below the shock, ϕ^- and maybe found by maximising $\dot{S}$ with respect to ϕ^-

$$\frac{\partial \dot{S}}{\partial \phi^-}=\frac{1}{\phi^- - \phi^+}\frac{\partial F}{\partial \phi^-}-\frac{F(\phi^-)-F(\phi^+)}{(\phi^- - \phi^+)^2}=0. \tag{8}$$

It is noteworthy that the shock speed is equal to $\lambda(\phi^-)$ and so the shock lies on a characteristic curve. Additionally we require that $\phi^- > \phi^+$ to maintain gravitational stability and we denote the fastest growing shock as $\dot{S}_*$. In a similar manner it is shown that the deposit growth rate must be given by the shock condition (7b) because otherwise the bed growth rate becomes unbounded as the volume fraction approaches ϕ_m.

Typical solutions for the characteristic curves are shown in Fig. 1a–c for a continuous dependence of the flux of particles, $F(\phi)$, upon the concentration, ϕ, as pioneered by Kynch (1952). Typically these flux functions are of the form $F=\phi(\phi_m-\phi)^n$ so that the flux vanishes as the maximum volume fraction is attained. The profiles feature shocks and rarefaction fans, as will be discussed below. Importantly this form of flux function has the consequence that the characteristic along which $\phi=\phi_m$ has vanishing gradient ($\lambda(\phi_m)=0$, provided $n>1$). Thus the suspension does not settle out to the maximum concentration within a finite time. Kynch foresaw this and sketched flux functions that avoided the problem, although he did not present an equation for a suitable flux. Various authors (Barton et al., 1992) have attempted to artificially modify the flux function so that finite settling times are predicted for vanishing flux as $\phi\to\phi_m$, whereas in this contribution we avoid the problem by choosing a discontinuous flux function as discussed previously, (3).

The characteristic profiles pictured in Fig. 1d–h, calculated using a hindered settling law (3) feature a combination of four

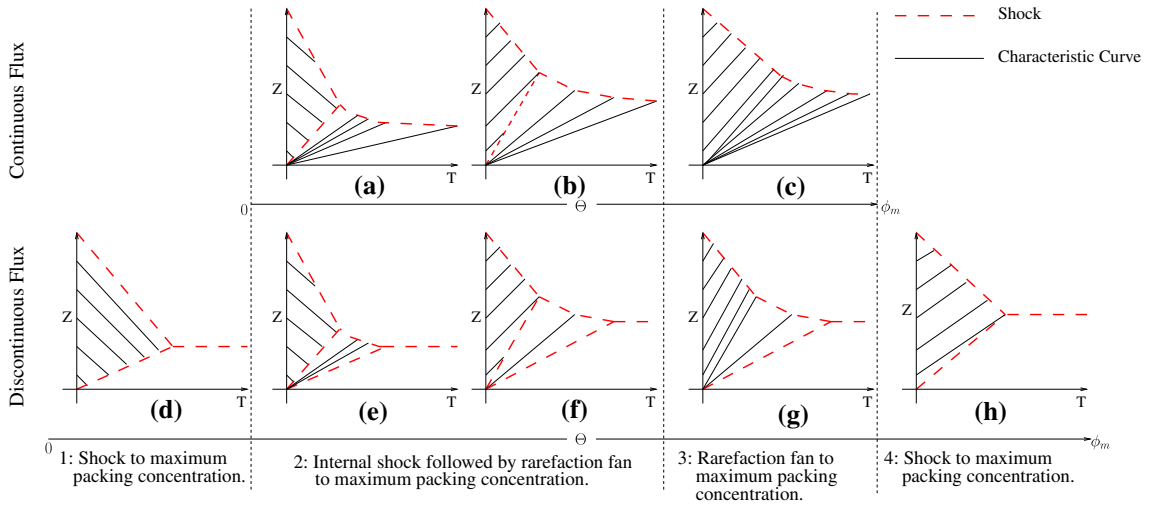

Fig. 1. Sketched characteristic curves for monodisperse settling with a continuous flux (a)–(c) and a discontinuous flux (d)–(h). The figures depict the possible structures of the solutions depending upon the initial volume fraction, Θ. The characteristic plane features characteristic curves, which are also contours of volume fraction (solid lines) and shocks, across which the volume fraction changes discontinuously (dashed lines).

different processes. Firstly, the location of the top interface defined as the separation between clear fluid and the suspension. Secondly, the location and growth rate of the top of the deposit, which is defined as the interface between the suspension below and at the maximum packing concentration. Third and fourthly are the existence of interior shocks or rarefaction fans in the characteristic curves.

The behaviour of the characteristic curves as the initial volume fraction Θ is increased is depicted in Fig. 1d–h and was reported by Auzerais et al. (1988). For low initial concentrations, the gradient of characteristics is negative and the shock speed of the interior shock, $\dot{S}_*$ is less than that of the shock speed to the maximum packing, $\dot{S}_m$, Fig. 1d. Increasing the initial concentration we find that there exists shocks over which the volume fraction jumps to some ϕ^-, less than ϕ_m. These arise because their shock speed is greater than the shock speed for a jump to the maximum packing concentration, ϕ_m. Thus the solutions feature two shocks, one from ϕ^+ to some $\phi^- < \phi_m$ and then after a rarefaction fan in which ϕ increases, followed by a further shock to the deposit. Further increasing Θ beyond $1/(n+1)$ reverses the direction of the characteristics, although the overall structure remains the same, see Fig. 1e-f. For still larger values of Θ, we find that the interior shock vanishes occurring at $\Theta = 2/(n+1)$, see Fig. 1g. For larger Θ the shock to the maximum packing overtakes the rarefaction fan (Fig. 1g). Following Auzerais et al. (1988), there are four settling regimes depicted in Fig. 1 and summarised in Fig. 2, which are determined, in terms of the total mass loading Θ and the concentration below the interior shock, ϕ^- (8), by the conditions

$$\left.\begin{array}{lllll} \text{Regime 1} & \dot{S}_m(\Theta) \geqslant \lambda(\Theta) & \dot{S}_m(\Theta) \geqslant \dot{S}_*(\Theta) & \Theta < \phi^- < \phi_m \\ \text{Regime 2} & \dot{S}_*(\Theta) \geqslant \dot{S}_m(\Theta) & \dot{S}_*(\Theta) \geqslant \lambda(\Theta) & \Theta < \phi^- < \phi_m \\ \text{Regime 3} & \lambda(\Theta) \geqslant \dot{S}_m(\Theta) & \nexists \dot{S}_* \text{ such that } \Theta < \phi^- < \phi_m & \\ \text{Regime 4} & \dot{S}_m(\Theta) \geqslant \lambda(\Theta) & \nexists \dot{S}_* \text{ such that } \Theta < \phi^- < \phi_m & \end{array}\right\}. \tag{9}$$

3. Sedimentation of bidisperse particle suspensions

We now extend the mathematical model to the sedimentation of bidisperse suspensions. To this end we denote the volume fraction and dimensionless settling velocity of class i of particles by ϕ_i and $\hat{w}_{si}$, in terms of variables, for which the flow depth h and the maximum terminal settling velocity have been used to render space and time scales dimensionless. Further, assuming that the particles are of uniform density and their terminal velocity in an unbounded fluid is given by Stokes' law, we find that the dimensionless slip velocity $\hat{w}_{pi}$ simplifies to the Richardson and Zaki viscosity modification multiplied by the square of the ratio of particle diameters $\hat{w}_{pi} = (1-\Phi)^{n-1}(D_i/D_2)^2$. We note that the analysis can be readily extended to incorporate particles of varying density, but at the cost of increased algebraic complexity (Bürger et al., 2000).

We find the following expressions of mass conservation for each particle species and for the interstitial fluid.

$$\frac{\partial \phi_i}{\partial T} + \frac{\partial}{\partial Z}(\phi_i \hat{w}_{si}) = 0 \quad \text{and} \quad \frac{\partial (1-\Phi)}{\partial T} + \frac{\partial}{\partial Z}\left(\hat{w}_f (1-\Phi)\right) = 0, \tag{10}$$

where $\Phi = \sum_i \phi_i$ denotes the total volume fraction of particulate. Given the slip velocity of each phase is written as $\hat{w}_{pi} = \hat{w}_{si} - \hat{w}_f$ we deduce, as shown by Masliyah (1979), that

$$\hat{w}_{si} = \hat{w}_{pi} - \sum_{j=1}^{2} \phi_j \hat{w}_{pj}. \tag{11}$$

To close this model we employ a model of the slip velocity in which the viscous drag, with the viscosity enhanced by a function of the total volume fraction of particulate, $\mu_e = \mu/(1-\Phi)^{n-1}$ is balanced by the submerged weight of the particles, provided that the total volume fraction is less than the maximum, ϕ_m. However, if the volume fraction exceed this maximum then it is assumed that the solid matrix supports the submerged weight and the slip velocity vanishes.

Thus in dimensionless form, the settling velocity of class i of particles is given by

$$\hat{w}_{si} = \begin{cases} \left(\hat{w}_{pi} - \sum_{i=1}^{2} \hat{w}_{pi}\phi_i\right) & \Phi \leqslant \phi_m \\ 0 & \Phi > \phi_m \end{cases}. \tag{12}$$

This formulation of bidisperse settling (12), by calculating the difference between the solid phase slip velocity and the surrounding fluid velocity is the extension of the monodisperse settling law (3) to polydisperse suspensions (Masliyah, 1979). Here it is assumed that ϕ_m is a constant, but this is not necessarily accurate as the packing density of polydisperse suspensions can exceed those of monodisperse suspensions (Sanders, 1980). The effect of a variable

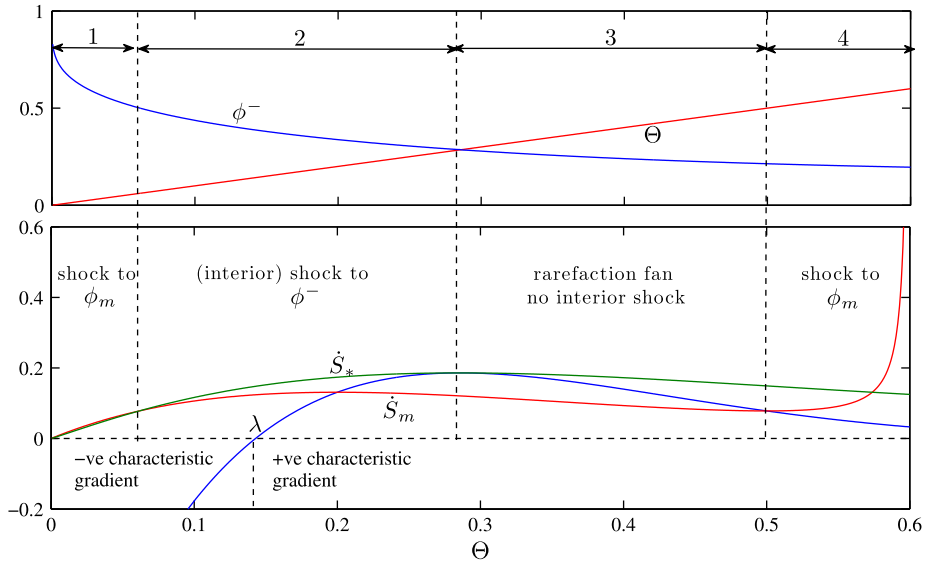

Fig. 2. The shock speeds $\dot{S}_*$ and $\dot{S}_m$, the characteristic velocity λ and the concentration below an interior shock ϕ^- satisfying condition (8), as functions of the total volume fraction Θ, for $n = 6$ and $\phi_m = 0.6$. This graphically displays the existence of the four settling regimes described by (9) and pictured in Fig. 1d–h.

ϕ_m is discussed in Appendix A, where we analyse the settling behaviour and deposit structure when the maximum packing becomes a function of particle size and concentration of each species.

By defining the flux per unit area of each class by $F_i = \phi_i \hat{w}_{si}$, we deduce the following coupled system of partial differential equation to govern the volume of the species of particles

$$\frac{\partial \phi}{\partial T} + K\frac{\partial \phi}{\partial Z} = 0 \quad \text{where} \quad \phi = \begin{pmatrix} \phi_1 \\ \phi_2 \end{pmatrix} \quad \text{and} \quad K = \begin{pmatrix} \frac{\partial F_1}{\partial \phi_1} & \frac{\partial F_1}{\partial \phi_2} \\ \frac{\partial F_2}{\partial \phi_1} & \frac{\partial F_2}{\partial \phi_2} \end{pmatrix}. \tag{13}$$

This system will be solved subject to initial conditions that the concentration of both species is vertically uniform and given by

$$\phi_1 = \alpha\Theta \quad \text{and} \quad \phi_2 = (1-\alpha)\Theta, \tag{14}$$

where $0 \leqslant \alpha \leqslant 1$ and Θ is the initial volume fraction of particulate. We note from the expressions of mass conservations that there will be an initial upward flux of the smaller particle (henceforth denoted as class 1) if

$$\hat{w}_{p1} < \frac{(1-\alpha)\Theta}{1-\alpha\Theta}. \tag{15}$$

The governing equations admit shocks, the speeds of which, $\dot{S}$, are given by

$$\dot{S}(T) = \frac{F_1^- - F_1^+}{\phi_1^- - \phi_1^+} = \frac{F_2^- - F_2^+}{\phi_2^- - \phi_2^+}, \tag{16}$$

where the superscripts denote evaluation above ($^+$) and below ($^-$) the shock, respectively. The characteristic form is found from the matrix representation of the mass conservation Eqs. (13) by evaluating the eigenvalues λ_i and left eigenvectors $\mathbf{L}^i = (L_1^i, L_2^i)$,

$$L_1^i\frac{\mathrm{d}\phi_1}{\mathrm{d}T} + L_2^i\frac{\mathrm{d}\phi_2}{\mathrm{d}T} = 0 \text{ on } \frac{\mathrm{d}Z}{\mathrm{d}T} = \lambda_i,$$

$$\lambda_{1,2} = \frac{1}{2}\left(\frac{\partial F_1}{\partial \phi_1} + \frac{\partial F_2}{\partial \phi_2}\right) \pm \frac{1}{2}\sqrt{\left(\frac{\partial F_1}{\partial \phi_1}\right)^2 + \left(\frac{\partial F_2}{\partial \phi_2}\right)^2 - 2\frac{\partial F_1}{\partial \phi_1}\frac{\partial F_2}{\partial \phi_2} + 4\frac{\partial F_1}{\partial \phi_2}\frac{\partial F_2}{\partial \phi_1}},$$

$$\mathbf{L}^{1,2} = \left(-\frac{\frac{\partial F_2}{\partial \phi_1}}{\frac{1}{2}\left(\frac{\partial F_1}{\partial \phi_1} - \frac{\partial F_2}{\partial \phi_2}\right) \pm \frac{1}{2}\sqrt{\left(\frac{\partial F_1}{\partial \phi_1}\right)^2 + \left(\frac{\partial F_2}{\partial \phi_2}\right)^2 - 2\frac{\partial F_1}{\partial \phi_1}\frac{\partial F_2}{\partial \phi_2} + 4\frac{\partial F_1}{\partial \phi_2}\frac{\partial F_2}{\partial \phi_1}}}, 1 \right) \tag{17}$$

where λ_1 and L_i^1 take the negative sign of the square root and λ_2 and L_i^2 the positive sign. The characteristic form (17) may be integrated to yield the Riemann invariants, which are constant along the characteristic curves. Unlike the Batchelor sedimentation model (Batchelor and Rensburg, 1984) the MLB model of settling velocities always results in real-valued eigenvalues and eigenvectors for characteristics. This can be demonstrated by showing the term

$$\left(\frac{\partial F_1}{\partial \phi_1}\right)^2 + \left(\frac{\partial F_2}{\partial \phi_2}\right)^2 - 2\frac{\partial F_1}{\partial \phi_1}\frac{\partial F_2}{\partial \phi_2} + 4\frac{\partial F_1}{\partial \phi_2}\frac{\partial F_2}{\partial \phi_1} \geqslant 0. \tag{18}$$

Using the settling velocity (12), where $\hat{w}_{pi}$ is the Stokesian settling velocity subject to the Richardson and Zaki (1954) effective viscosity modification, we can reduce (18) to

$$\left(\left(\frac{D_1}{D_2}\right)^2(\phi_1(n+1)-1) - (\phi_2(n+1)-1)\right)^2 + 4\left(\frac{D_1}{D_2}\right)^2\phi_1\phi_2(n+1)^2 \geqslant 0, \tag{19}$$

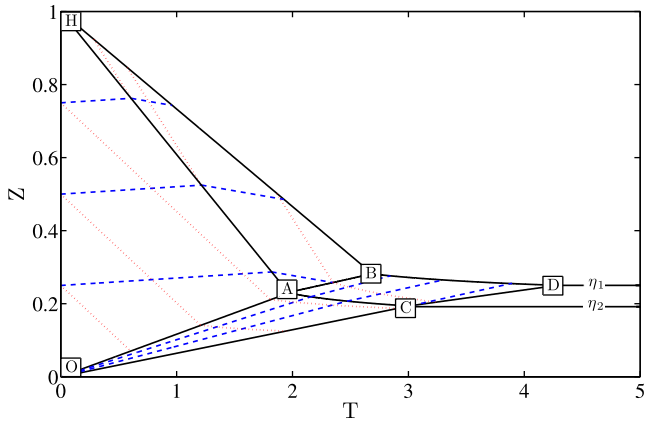

Fig. 3. The characteristic plane for bidisperse settling with shocks depicted with a solid line, λ_1-characteristics with a dotted line and λ_2-characteristics with a dashed line. The parameters used to construct this plot were $n = 6$, $D_1/D_2 = 3/4$, $\phi_m = 0.6$, $\Theta = 0.15$ and $\alpha = 0.5$.

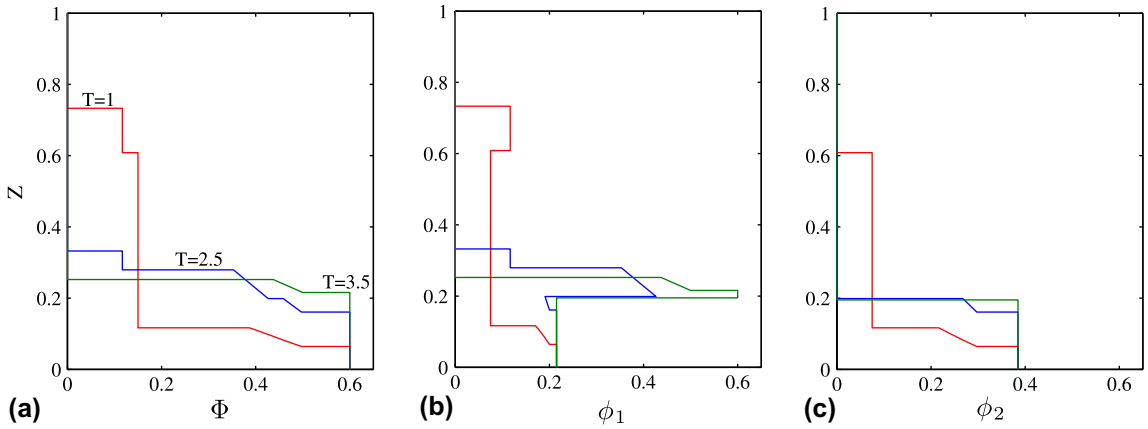

Fig. 4. (a) The total volume fraction, $\Phi(Z,T)$; (b) volume fraction, $\phi_1(Z,T)$; and (c) volume fraction, $\phi_2(Z,T)$ as functions of the dimensionless height at $T = 1.0, 2.5, 3.5$. Times were chosen to coincide with different behaviours in the regions of the characteristic plane depicted in Fig. 3. The curves at $T = 1$, $T = 2.5$ and $T = 3.5$ capture the interior shock and the initial segregation of some of the smaller particles from the suspension (respectively region *OAH* and *ABH*); the rarefaction fans of both the monodisperse segregate and the bidisperse suspension (respectively region *OAC* and *ABCD*); and the final deposition of the monodisperse phase of smaller particles (η_1 to η_2). This bidisperse sedimentation problem is characterised by parameter values $n = 6$, $D_1/D_2 = 3/4$, $\phi_m = 0.6$, $\Theta = 0.15$ and $\alpha = 0.5$.

which can be seen to always be strictly greater than or equal to zero. Thus the system can always be treated as a hyperbolic set of equations. Basson et al. (2009) provide a different proof of hyperbolicity for a more general system, where n, the enhanced viscosity exponent, is allowed to vary with particle diameter.

We may construct analytical solutions to this system of equations by exploiting the form of the characteristic curves and by identifying the location of shocks. We illustrate the solution for a particular example with parameter values $n = 6$, $D_1/D_2 = 3/4$, $\phi_m = 0.6$, $\Theta = 0.15$ and $\alpha = 0.5$, presented in Fig. 3. There are six regions within this figure; *OAH* is the region within which both volume fractions are equal to their initial values; *OAC* is a rarefaction fan containing particles of both species; and the area under η_2 is deposit formed by a mixture of both particle species. The upper regions *ABH*, *ABCD* and the area between η_1 and η_2 are absent of the heavier particles. Forced by the settling velocity of the heavier particle, region *ABH* is of constant concentration and region *ABCD* is the continuation of the rarefaction fan. The area between η_1 and η_2 is deposit entirely consisting of the lighter particles of the initial suspension.

The figure shows that the solution features a number of shocks, lying along curves *OA*, *OC*, *HA*, *HB*, *AB*, *AC*, *BD* and *CD*. We use the interior shock along *OA* to classify the problem as belonging to regime 2, as in the monodisperse case, see Fig. 1. Settling regimes in the bidisperse case are described more completely by Fig. 5 and in Section 3.1. The evolution of some of these curves is straightforward: the curves *HA* and *AC* de-mark the upper limit of the region within which the larger particles (class 2) are found. The rate of change of the position along these curves is the settling velocity $\dot{w}_{s2}$, which is a function of the local volume fractions of both species. Likewise the curves *HB* and *BD* demarcate the upper extent of the smaller particles (class 1) and thus their rates of change is $\dot{w}_{s1}$, which here is only a function of ϕ_1 as these curves are boundaries to regions absent of suspended larger particles ($\phi_2 = 0$). Within the region *OAH*, both volume fractions are constant and equal to their initial conditions. Thus below this uniform region, *OAC* is a rarefaction fan within which the λ_2-characteristics are straight lines emanating from the origin. This region is separated from the adjoining uniform region by a shock, *OA*, the speed of which is maximised, by the same arguments discussed in Section 2. By viewing (16a, b) as expressions for $\dot{S}(\phi_1^-, \phi_2^-)$ and by seeking conditions for when $\partial\dot{S}/\partial\phi_1^- = 0$ and $\partial\dot{S}/\partial\phi_2^- = 0$, subject to enforcing the equality of (16a) and (16b), we find that the shock speed along *OA*, $\dot{S}_*$, satisfies

$$\left(\frac{\partial F_1^-}{\partial \phi_1^-} - \dot{S}_*\right)\left(\frac{\partial F_2^-}{\partial \phi_2^-} - \dot{S}_*\right) = \frac{\partial F_2^-}{\partial \phi_1^-}\frac{\partial F_1^-}{\partial \phi_2^-}. \tag{20}$$

Hence the speed of the shock is identical to the characteristic speed, λ_2 and so the shock lies on a characteristic curve. Within the rarefaction fan, *OAC*, we calculate the Riemann invariant that remains constant along the λ_1-characteristics. This is given by $\mathrm{d}\phi_1/\mathrm{d}\phi_2 = -L_2^1/L_1^1$, from which we deduce that $\phi_2 = G(\phi_1)$ for some determined function G. From (17) it can then be deduced that on λ_2-characteristics within the fan *OAC*, both volume fractions are constant if $L_1^1 L_2^2 - L_2^1 L_1^2 \neq 0$ and this latter condition is necessarily held for this system of governing equations. We calculate the lower boundary to the rarefaction fan, curve *OC*, as a shock over which the total volume fraction jumps to ϕ_m, the value corresponding to maximum packing. This boundary is also a λ_2-characteristic that starts at the origin. The shock speed along *OC*, after a rarefaction fan, is found by maximising the bed growth rate, given by

$$\dot{S}_m = \frac{-F_1^+}{\phi_1^- - \phi_1^+} = \frac{-F_2^+}{\phi_2^- - \phi_2^+} = \lambda_2, \tag{21}$$

together with $\phi_2^+ = G(\phi_1^+)$ and $\phi_1^- + \phi_2^- = \phi_m$. If the shock to the maximum packing concentration does not occur after a rarefaction fan it may be found from (21), where ϕ_1^+, ϕ_2^+ are given by the initial

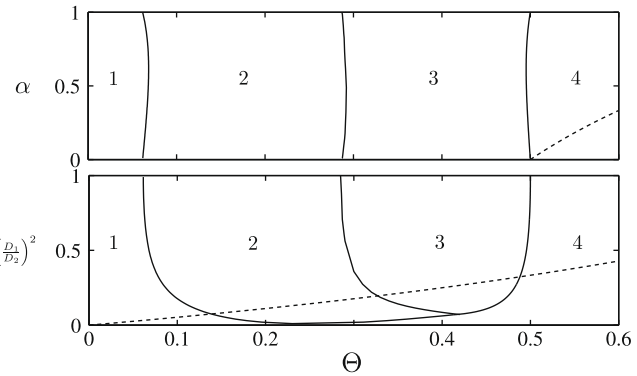

Fig. 5. The settling regimes (1–4) of bidisperse settling from uniform initial conditions as a function of the initial volume fraction Θ, the proportion of smaller particles, α and the relative Stokesian settling velocities $(D_1/D_2)^2$ for a discontinuous settling law (12) with $n = 6$, $\phi_m = 0.6$. In (a) $(D_1/D_2)^2 = 0.5$ and in (b) $\alpha = 0.5$. The dashed line depicts the interface in the phase space below which the smallest particle class is carried upwards by the return flux of water.

concentration and $\phi_1^- + \phi_2^- = \phi_m$. Finally the shock AC is constructed as the boundary to the rarefaction region over which the volume fraction of the larger particles (class 2) jumps from their value within the fan OAC to zero. Thus the speed of the shock is $\hat{w}_{s2}$.

This structure of characteristic curves produces rather complicated profiles of the volume fraction at various instants of time. In Fig. 4 we depict the volume fractions of both species at three times during their sedimentation, noting that they exhibit a number of evolving discontinuities.

3.1. Settling behaviour of bidisperse suspensions

The pattern of sedimentation of a bidisperse suspension and the structure of the characteristic curves is determined by the initial total volume fraction, Φ, the ratio of the settling velocities, $(D_1/D_2)^2$ and the initial proportion of each class of particle, α. Above we have described in detail the evolution of the suspension for particular values of these parameters, which features a shock to the maximum packing fraction, an internal shock (implying it belongs to settling regime 2, Fig. 5) and a rarefaction fan (see curves OC, OA and region OAC in Fig. 3). As the parameters vary, the magnitude of these shocks change and, in analogous manner to monodisperse suspensions, we can identify four settling regimes.

Settling regimes 1 and 4 exhibit a direct shock to the maximum packing concentration, where regime 1 is at very low initial particle concentration and regime 4 is at very high initial particle concentration. Regime 2 exhibits an interior shock followed by a rarefaction fan, see Fig. 3, regime 3 is analogous to regime 2 but

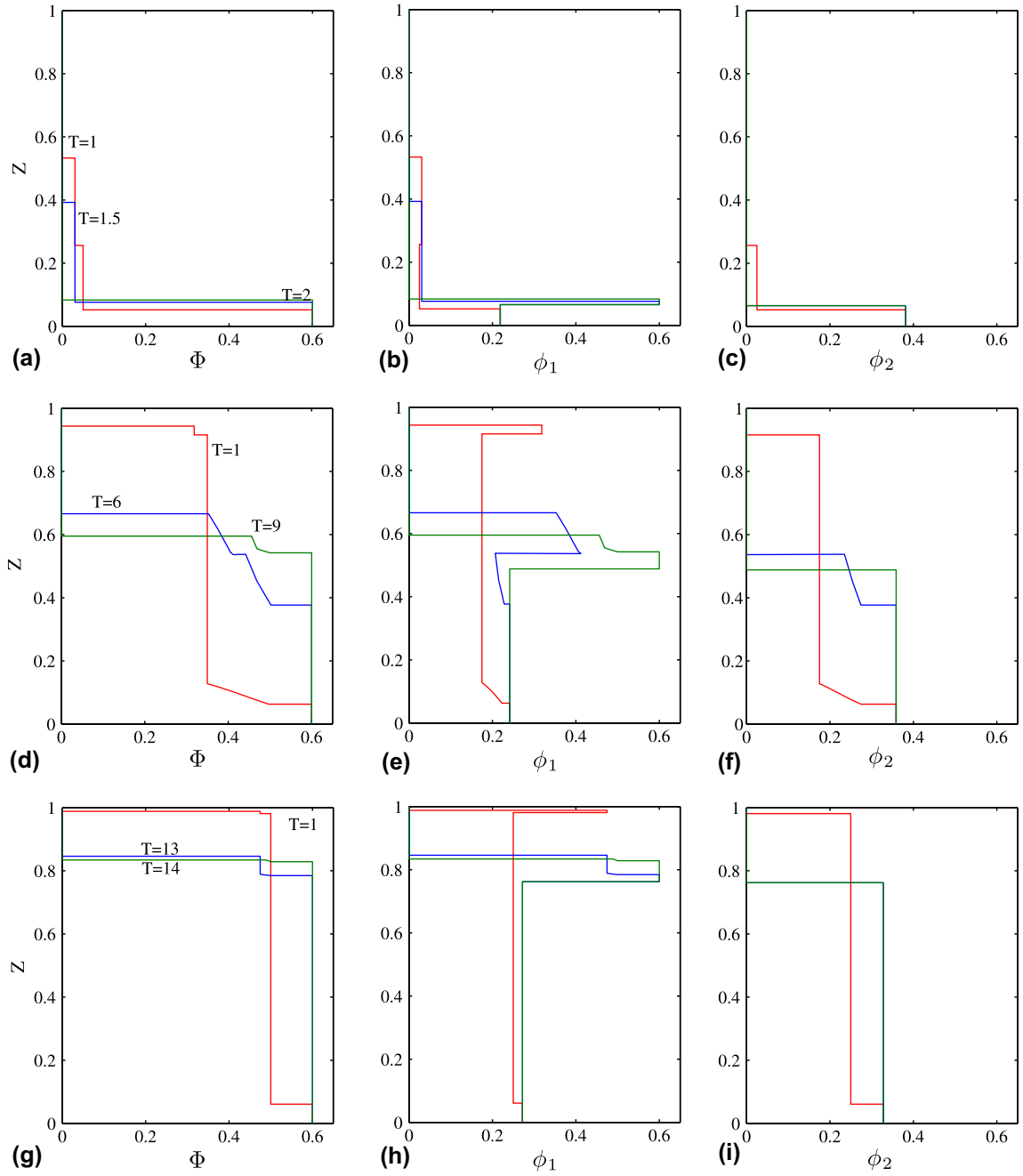

Fig. 6. The evolution of the total volume fraction, $\Phi(Z,T)$ and particle volume fractions $\phi_1(Z,T)$ and $\phi_2(Z,T)$ as functions of the dimensionless height for varying mass loadings; $\Theta = 0.05$ (a), (b) and (c); $\Theta = 0.35$ (d), (e) and (f); $\Theta = 0.5$ (g), (h), (i). The different mass loadings correspond to settling regimes 1 ($\Theta = 0.05$), 3 ($\Theta = 0.35$) and 4 ($\Theta = 0.5$), as shown in Fig. 5. Evolution from settling regime 2 is shown in Fig. 4. Here $D_1/D_2 = 3/4$, $\alpha = 0.5$, $n = 6$ and $\phi_m = 0.6$.

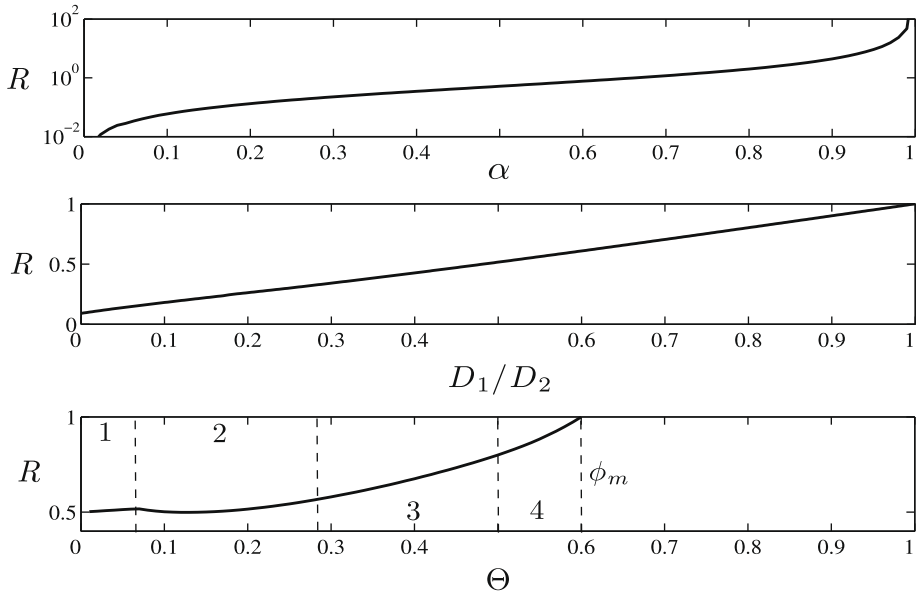

Fig. 7. The mixing ratio in the deposit, R, as a function of the total volume fraction Θ, the ratio of settling velocities $(D_1/D_2)^2$ and initial proportion of smaller particles, α. Unless depicted otherwise the parameter values for the bidisperse settling are given by $\Theta = 0.2,\ (D_1/D_2)^2 = 0.5,\ \alpha = 0.5$. The settling regimes that arise as a function of the total volume fraction are denoted $1 \rightarrow 4$ (see Fig. 5). For the figure depicting the variation of R with $(D_1/D_2)^2$ there is a settling regime change from $1 \rightarrow 2$ which is not clearly visible on these scales ($(D_1/D_2)^2 \approx 0.018$).

has no interior shock (along the arc OA in Fig. 3). Transition between the regimes 1 to 4 occurs with increasing the initial volume fraction, Θ. The concentration of the monodisperse region of smaller particles (*ABH* and *ABCD* in Fig. 3) is directly forced by the discontinuity in particle concentration caused by the difference in settling velocity between particle classes. Regions of downwards (upper) and upwards (lower) flux of the lightest particles are separated by the dashed line in Fig. 5. These settling regimes are analogous to those depicted in Fig. 1 for monodisperse suspensions (Auzerais et al., 1988). As in (9), boundaries between regimes are described in terms of the total mass loading Θ, the interior shock speed $\dot{S}_*$ and shock speed to the maximum packing concentration $\dot{S}_m$, positive characteristics λ_2 and the total concentration below an interior shock Φ^-,

$$\left.\begin{array}{llll} \text{Regime 1} & \dot{S}_m(\Theta) \geqslant \lambda_2(\Theta) & \dot{S}_m(\Theta) \geqslant \dot{S}_*(\Theta) & \Theta < \Phi^- < \phi_m \\ \text{Regime 2} & \dot{S}_*(\Theta) \geqslant \dot{S}_m(\Theta) & \dot{S}_*(\Theta) \geqslant \lambda_2(\Theta) & \Theta < \Phi^- < \phi_m \\ \text{Regime 3} & \lambda_2(\Theta) \geqslant \dot{S}_m(\Theta) & \nexists \dot{S}_* \text{ such that } \Theta < \Phi^- < \phi_m & \\ \text{Regime 4} & \dot{S}_m(\Theta) \geqslant \lambda_2(\Theta) & \nexists \dot{S}_* \text{ such that } \Theta < \Phi^- < \phi_m & \end{array}\right\}. \tag{22}$$

In Fig. 5 it is observed that changing the total volume fraction in suspension and to a lesser extent the ratio of Stokesian settling velocities (given by particle sizes) will greatly affect which settling regime is observed. Varying the proportion of each type of sediment only weakly affects the settling behaviour of a bidisperse suspension. The evolution of concentration profiles for settling regimes 1, 3 and 4 is shown in Fig. 6, sedimentation belonging to regime 2 was shown in Fig. 4. In these figures sedimentation problems from regime 1 and 4 can be seen to have shocks to the maximum packing concentration, regime 2 has a shock followed by a rarefaction fan and then another shock to the maximum packing concentration whereas regime 3 type sedimentation problem has a rarefaction fan followed by a shock to the maximum packing concentration. These characteristic profiles can all be observed at $T = 1$, which is plotted for each problem (see Fig. 6).

3.2. Deposit structure from bidisperse suspensions

In many naturally-occurring situations the composition of the deposit that arises from sedimentation is of interest. It is possible to calculate this exactly for this bidisperse suspension using the characteristic solutions presented above. It is evident that from vertically uniform initial conditions the deposit will be composed of a region of mixed large and small particles, in which the ratio of the smaller to the larger grains is denoted by $R = \phi_1/\phi_2$, overlain by a layer of purely finer grains. This mixed layer persists over some depth, $0 < z < \eta_2$, while the layer of fine grains is found for $\eta_2 < z < \eta_1$ (see Fig. 3). The ratio, R is determined by the ratio of the fluxes of each species at the top of the developing deposited layer (along the arc *OC* in Fig. 3). As was shown from the characteristic equations the particle concentration and therefore particle flux is constant along this arc until all the larger particles are deposited and thus R is also a constant in the region of the deposit between 0 and η_2.

In Fig. 7 we plot the dependence of R upon the parameters α, $(D_1/D_2)^2$ and Θ. From this figure we note that for fixed α and $(D_1/D_2)^2$ there is a non-monotonic variation of the ratio of particles with the total initial volume fraction. This arises due to the complicated settling behaviour that is found as the volume fraction changes (regimes 1–4), which feature internal shocks and rarefactions, thus altering the vertical distribution of the suspended particles and consequently affecting the composition of the deposit.

4. Summary and Conclusions

Analytical solutions have been constructed to reveal the sedimentation behaviour of initially uniform monodisperse and bidisperse suspensions. This work has generalised the pioneering study of Kynch (1952) to mixtures of particles sizes (and densities) and has calculated the evolving state of the suspension, in addition to the composition of the deposit, as settling occurs through otherwise quiescent fluid. Depending on the initial volume fraction, and for bidisperse suspensions the initial relative proportions and settling velocities, these solutions feature a rich structure of

shocks and rarefactions. We have shown how to classify the settling behaviour in to one of four regimes, dependent on the governing parameters and that this classification may be used for both mono and polydisperse suspensions. Additionally we have shown that bidisperse suspensions generate a deposit in which there is a region of mixed particles of constant composition, overlain by a layer composed only of the particles with the smaller settling velocity.

From this study we may explain two observations found in the experimental results reported by Amy et al. (2006). First they identified an ungraded region at the base the deposit. We may interpret this as due to the vertically uniform initial distribution of the sediment in the experiments. Such initial conditions give rise to constant fluxes of each particle type into the shock that marks the top of the growing deposit. Second they found that the size of the ungraded region, when normalised with respect to final deposit depth, grew as the total initial volume fraction was increased. This may be explained by noting that the ungraded region forms until the largest particle has been completely deposited, where the settling velocity of the largest particle class is significantly reduced as total volume fraction is increased (12) but that the speed of the shock to the maximum packing concentration is only weakly affected by total volume fraction.

Acknowledgements

This work was supported by the Natural Environment Research Council under Grant number [NER/S/A/2006/14067]. Lawrence Amy, Esther Sumner and Peter Talling are thanked for constructive and informative comments.

Appendix A. Maximum packing laws

In this appendix we extend the analysis of bidisperse settling to incorporate a variable maximum packing concentration, which is greater than the maximum packing value of a monodisperse suspension, reflecting the packing of smaller grains into the space between larger grains. In what follows we denote the total maximum packing of a bidisperse suspension by $\phi_b = \phi_1 + \phi_2$ while ϕ_m remains the maximum packing of a monodisperse suspension.

It is well known that when considering binary or polydisperse mixtures of spheres that the maximum packing value can be increased, see for example Kansal et al. (2002), Sanders (1980) and Shapiro and Probstein (1992). However although the random loose packing of equal spheres is fairly well understood, see Kansal et al. (2002) and references therein, it is not as well established how the random loose packing of polydisperse mixtures is dependent on the individual volume fractions of each class of particles and the relative diameters of the particles.

It has been established experimentally that the maximum packing concentration of a bidisperse mixture of particles tends to the maximum packing of a monodisperse mixture of particles as the proportion of the deposit occupied by the largest or smallest particle class vanishes (Shapiro and Probstein, 1992). Further it has been shown, see for example Shapiro and Probstein (1992), Kansal et al. (2002), that decreasing the ratio of particle size, (D_1/D_2), increases the maximum packing.

To illustrate the effects of this enhanced packing on bidisperse bulk settling, we introduce the following simple expression for the maximum packing fraction, ϕ_b, that allows for packing fractions in excess of ϕ_m when there is a mixture of particle sizes

$$\phi_b = \phi_m + \phi_1\phi_2\left(1 - \frac{D_1}{D_2}\right)\phi_m. \tag{A.1}$$

This expression shares some features with the formulation suggested by Kansal et al. (2002) and permits an illustrative calculation of bidisperse sedimentation and deposit formation using the analytical techniques employed in the main body of the paper. We note that when the particles are of the same size $(D_1 = D_2)$ and when one of the particles species is absent ($\phi_1 = 0$ or $\phi_2 = 0$), the packing fraction of the deposit reduces to monodisperse value. Improved expressions may be substituted in place of (A.1) as they become available.

We now employ this model of bidisperse packing and calculate the sedimentation from an initially well mixed suspension with $\phi_1(Z,0) = \phi_2(Z,0) = 0.075$ and for parameters $n = 6$, $D_1/D_2 = 3/4$ and $\phi_m = 0.6$. (Settling from these initial conditions with these parameter values was described in detail in Section 3 and the characteristic plane was plotted in Fig. 3.) With the enhanced packing in the deposit, we find that the solutions for the volume fraction of each species remain rather similar to the results derived in Section 3, with the same structure of shocks and rarefaction fans. This is most readily seen in the plot of the characteristic plane (Fig. A.1). Here we note that the main differences is the reduction in the bed growth rate, which occurs due to the higher packing fraction in the deposit. For this case, we find that the bed volume fraction is increased from 0.6 to 0.6129 during the phase of the settling in which it comprises both particles (see Fig. A.1). Also during this phase, although the volumes fractions of both species increase, the ratio of the particle volume fractions, $R = \phi_1/\phi_2$ is somewhat

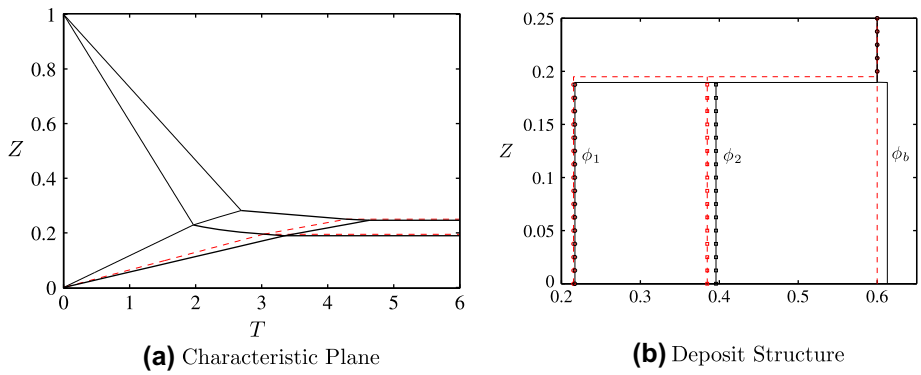

(a) Characteristic Plane **(b)** Deposit Structure

Fig. A.1. (a) The characteristic plane when using the enhanced packing fraction (A.1) for $n = 6$, $D_1/D_2 = 3/4$, $\phi_m = 0.6$, $\Theta = 0.15$ and $\alpha = 0.5$, showing only the locations of the shocks (solid lines). Also shown is the location of the shocks when $\phi_b = \phi_m$ (dashed lines). (b) The volume fractions of the particle classes, ϕ_1 (circles) and ϕ_2 (squares), and the total volume fraction, ϕ_b, as a function of height, calculated using an enhanced maximum packing fraction (solid) and a constant maximum packing fraction (dashed). For both calculations, there is initially a bidisperse deposit of both species, which is then overlain by deposit, consisting only of ϕ_1. The total depth of the depth is 0.2461 and 0.25 for the enhanced and constant maximum packings, respectively.

reduced, indicating that the fraction of fine particles is reduced. Finally we note that the time for the all of the suspension to settle out is increased, which occurs due to the reduced bed growth rate.

This illustrative calculation shows that the results presented in this paper may be readily generalised to account for the enhanced packing fractions of bidisperse deposits and that the overall structure of the solution may remain invariant under such generalisations.

References

Amy, L., Talling, P.J., Edmonds, V.O., Sumner, E.J., Leseur, A., 2006. An experimental investigation of sand–mud suspension settling behaviour: implications for bimodal mud content of submarine flow deposits. Sedimentology 53, 1411–1434.

Auzerais, F.M., Jackson, R., Russel, W.B., 1988. The resolution of shocks and the effects of compressible sediments in transient settling. J. Fluid Mech. 195, 437–462.

Barton, N.G., Li, C.H., Spencer, S.J., 1992. Control of a surface of discontinuity in continuous thickness. J. Aust. Math. Soc., Ser. B – Appl. Math. 33, 269–289.

Basson, D.K., Berres, S., Bürger, R., 2009. On models of polydisperse sedimentation with particle-size-specific hindered-settling factors. J. Appl. Math. Model., 33 1815–1835.

Batchelor, G.K., 1967. An Introduction to Fluid Dynamics. Cambridge University Press. pp. 615.

Batchelor, G.K., 1982. Sedimentation in a dilute polydisperse system of interacting spheres. Part 1. General theory. J. Fluid Mech. 119, 379–408.

Batchelor, G.K., Rensburg, R.W.J.V., 1984. Structure formation in bidisperse sedimentation. J. Fluid Mech. 166, 379–407.

Bürger, R., Concha, F., Fjelde, K.K., Karlsen, K.H., 2000. Numerical simulation of the settling of polydisperse suspensions of spheres. Powder Technol. 113, 30–54.

Bürger, R., Garcia, A., Karlsen, K.H., Towers, J.D., 2008. A family of numerical schemes for kinematics flows with discontinuous flux. J. Eng. Math. 60, 387–425.

Cheung, M.K., Powell, R.L., McCarthy, M.J., 1994. Sedimentation of non-collidal bidisperse suspensions. AIChE J. 42, 271–276.

Cuthbertson, A., Dong, P., King, S., Davies, P., 2008. Hindered settling velocity of cohesive/non-cohesive sediment mixtures. Coast. Eng. 55, 1197–1208.

Davis, R.H., Gecol, H., 1994. Hindered settling function with no empirical parameters for polydisperse suspensions. AIChE J. 40, 570–575.

Funamizu, N., Takakuwa, T., 1996. A minimal potential energy model for predicting stratification pattern in binary and ternary solid–liquid fluidized beds. Chem. Eng. Sci. 51, 341–351.

Hoyos, M., Bacri, J.C., Martin, J., Salin, D., 1994. A study of the sedimentation of noncolloidal bidisperse, concentrated suspensions by an acoustic technique. J. Phys. Fluids 6, 3809–3817.

Kansal, A.R., Torquato, S., Stillinger, F.H., 2002. Computer generation of dense polydisperse sphere packings. J. Chem. Phys. 117, 8212–8218.

Koo, S., 2009. Sedimentation velocities of bidisperse suspensions. J. Ind. Eng. Chem. 14, 679–686.

Kynch, G.J., 1952. A theory of sedimentation. Trans. Faraday Soc. 48, 166–176.

Lockett, M.J., Al-Habbooby, H.M., 1973. Differential settling by size of two particle species in a liquid. Chem. Eng. Res. Des. 51, 281–292.

Lockett, M.J., Bassoon, K.S., 1979. Sedimentation of binary particle mixtures. J. Powder Technol., 17–24.

Masliyah, J.H., 1979. Hindered settling in a multi-species particle system. Chem. Eng. Sci. 34, 1166–1168.

Richardson, J.F., Zaki, W.N., 1954. The sedimentation of a suspension of uniform spheres under conditions of viscous flow. Chem. Eng. Sci. 3, 65–78.

Sanders, J.V., 1980. Close-packed structures of sphers of two different sizes I. Observations on natural opal. Philos. Mag. A 42, 705–722.

Selim, M.S., Kothari, A.C., Turian, R.M., 1983. Sedimentation of multisized particles in concentrated suspensions. J. AIChE 29, 1029–1038.

Shapiro, A.P., Probstein, R.F., 1992. Random packings of spheres and fluidity limits of monodisperse and bidisperse suspensions. Phys. Rev. Lett. 68, 1422–1425.

Whitham, G.B., 1974. Linear and Nonlinear Waves. Wiley-Interscience, New York.

Xue, B., Sun, Y., 2002. Modeling of sedimentation of polydisperse spherical beads with a broad size distribution. J. Chem. Eng. Sci. 58, 1531–1543.